Metabolic Brain Disease (2025) 40:157
https://doi.org/10.1007/s11011-025-01589-8

RESEARCH

Sodium butyrate alleviates spinal cord injury via inhibition of NLRP3/Caspase-1/GSDMD-mediated pyroptosis

Yanru Cui[1] · Qiuyu Cen[1] · Jing Feng[1] · Juanfang Wei[2] · Linjie Wang[3] · Cong Chang[4] · Rizhao Pang[3] · Junyu Wang[1] · Anren Zhang[1]

Received: 16 November 2024 / Accepted: 18 March 2025 / Published online: 24 March 2025

Abstract

NOD-like receptor protein 3 (NLRP3)/cysteinyl aspartate-specific proteinase 1 (Caspase-1)/gasdermin D (GSDMD)-mediated pyroptosis is linked to spinal cord injury (SCI) pathogenesis. The levels of short-chain fatty acids (SCFAs), especially butyric acid, are significantly altered after SCI. Sodium butyrate (NaB) has anti-inflammatory effects on SCI; however, its effect on pyroptosis is unknown. The aim of this study was to determine the role of NaB in SCI functional recovery and its effect on NLRP3/Caspase-1/GSDMD-mediated pyroptosis. SCI model rats were established using aneurysm clips. After SCI, rats were administered NaB (300 mg/kg) via gavage. SCFAs in faeces were measured using gas chromatography-mass spectrometry. Motor function recovery was assessed using cylinder rearing and grooming tests. Histopathological analysis was performed using haematoxylin-eosin staining, transmission electron microscopy, and terminal deoxynucleotidyl transferase dUTP nick-end labelling. The expression of proteins associated with pyroptosis signalling pathways was analysed using enzyme-linked immunosorbent assay, western blotting, and immunohistochemistry. SCFAs levels, particularly butyric acid, significantly decreased after SCI. NaB treatment promoted forelimb motor function recovery and attenuated pathological SCI. NaB also decreased spinal pro-inflammatory factors (interleukin-18 and interleukin-1β) and downregulated pyroptosis-related proteins, including NLRP3, apoptosis-associated speck-like protein, Caspase-1, and GSDMD. NaB inhibits NLRP3/Caspase-1/GSDMD-mediated neuronal pyroptosis and inflammation, exerting protective and therapeutic effects in SCI, suggesting NaB as an effective SCI treatment.

Highlights

SCFAs levels (including butyric acid) were reduced after SCI.
NaB improved motor function after SCI.
NaB inhibited NLRP3/Caspase-1/GSDMD-mediated neuronal pyroptosis and inflammation.

Keywords Sodium butyrate · Neuroinflammation · Pyroptosis · Spinal cord injury

Yanru Cui, Qiuyu Cen and Jing Feng are co-first authors and contributed equally to this work.

✉ Rizhao Pang
przprz17@126.com

✉ Junyu Wang
wjy03150618@163.com

✉ Anren Zhang
anren0124@tongji.edu.cn

Yanru Cui
1219959904@qq.com

[1] Department of Rehabilitation Medicine, Shanghai Fourth People's Hospital Affiliated to Tongji University, Shanghai, China

[2] College of Physical Education and Health, Geely University of China, Chengdu, China

[3] Department of Rehabilitation Medicine, General Hospital of Western Theater Command, Chengdu, China

[4] Chengdu Eighth People's Hospital (Geriatric Hospital of Chengdu Medical College), Chengdu, China

Introduction

Spinal cord injury (SCI) is a severe injury to the central nervous system, often resulting in motor dysfunction (Anjum et al. 2020). The World Health Organization reports an incidence of 40–80 cases per million people worldwide, with approximately 250,000–500,000 new cases annually. Treatment costs per patient range from US$1 to US$5 million, depending on injury location and severity (Courtine and Sofroniew 2019), imposing a significant economic burden on the patient's family and society. Methylprednisolone is a drug commonly used in the treatment of acute SCI, and its primary mechanism of action is to bind with glucocorticosteroid receptors to prevent nuclear translocation of pro-inflammatory transcription factors (Chio et al. 2021). However, current methods of methylprednisolone administration are largely inefficient, as high doses of methylprednisolone are associated with serious side effects, such as pneumonia, infection, corticosteroid myopathy, and gastrointestinal bleeding (Song et al. 2019). Therefore, it is essential to actively explore new strategies for the treatment of SCI. Primary SCI can cause varying degrees of spinal cord shock, contusions, vascular rupture, altered vascular permeability, and axonal rupture (Liu et al. 2021a). Secondary injuries develop over days to weeks, including oedema, ischemia, excitotoxicity, electrolyte imbalances, free radical production, inflammatory responses, and cell death (Rowland et al. 2008). Addressing the widespread cell death triggered by secondary injury is a major challenge in SCI repair (Gong et al. 2022).

Pyroptosis, a novel programmed inflammatory cell death characterised by the formation of transmembrane pores, swelling of cells and rupture, and release of many inflammatory factors (Wu et al. 2021), is closely associated with the pathological mechanisms of SCI (Yin et al. 2022). NOD-like receptor protein 3 (NLRP3)/cysteinyl aspartate specific proteinase 1 (Caspase-1)/gasdermin D (GSDMD) is a classical pathway of pyroptosis (Su et al. 2023), NLRP3 activation leads to inflammasome formation, and Caspase-1 activation, which activates pro-inflammatory factors, such as interleukin-1β (IL-1β) and interleukin-18 (IL-18), and cleaves GSDMD to form cell membrane pores, ultimately inducing cell death and exacerbating SCI (Liu et al. 2021b). Pyroptosis after SCI causes excessive cellular inflammatory injury and aggravates glial and neuronal cell death, severely impeding the functional recovery of damaged nerves (Hu et al. 2020). Therefore, actively exploring therapeutic methods to inhibit pyroptosis is an effective strategy for alleviating damage secondary to SCI.

Alterations in the gut microbiota are closely associated with the development of pyroptosis. Dysbiosis leads to an increase in pathogen-associated molecular patterns, which subsequently activate inflammasome-mediated pyroptosis (Zhang et al. 2024; Huang et al. 2022). Recent evidence suggests that intestinal microbiota disruption is associated with neuroinflammation and motor dysfunction after SCI (Kigerl et al. 2016; Jing et al. 2021). SCI alters the intestinal microbiota, reducing bacterial diversity, increasing pathogenic or pro-inflammatory bacteria, and decreasing short-chain fatty acids (SCFAs)-producing bacteria, leading to gut dysfunction and exacerbated inflammatory responses, thus affecting motor function recovery (Bazzocchi et al. 2021; Kigerl et al. 2016). Our previous study showed altered intestinal microbiota composition after SCI, with a significant decrease in butyrate-producing bacteria (*Fusobacterium*) in patients with SCI compared to normal controls (Pang et al. 2022). SCFAs, metabolites of the intestinal microbiota, can enter somatic circulation and cross the blood–brain barrier, affecting brain function in healthy and diseased organisms (Sadler et al. 2020). Acetic, propionic, and butyric acid levels are significantly downregulated in patients with SCI. SCFAs faecal levels in patients with SCI at different stages of injury showed different characteristics, and supplementation with SCFAs significantly improved motor function, reduced inflammation, and enhanced neuronal survival in SCI mice (Jing et al. 2023). Butyric acid, one of the SCFAs, exhibits a variety of effects, including anti-inflammatory, antioxidant, and immune system modulation, which are essential for maintaining host health (Huang et al. 2023; Berni Canani et al. 2012). Sodium butyrate (NaB) is the form of sodium salt of butyric acid commonly used in pharmacological studies (Bourassa et al. 2016). In a mouse model of T6-T7 spinal cord clamp injury, NaB intervention significantly ameliorates histopathological changes after SCI and promotes motor function recovery while inhibiting the nuclear factor-κB (NF-κB) pathway activation and decreasing inflammatory factors (tumour necrosis factor-α and IL-1β) (Lanza et al. 2019). Another study demonstrated that NaB reduces pyroptosis by inhibiting the Caspase-1/GSDMD pathway, ameliorating glomerular endothelial cell injury (Gu et al. 2019). These studies suggest that the intestinal microbiota metabolites, SCFAs (particularly butyric acid), could be a potential treatment option for SCI. However, the effects of NaB on pyroptosis after SCI remain unknown. In this study, we aimed to investigate the role of NaB in pyroptosis following SCI by establishing a rat model of SCI.

Methods

Animals

Healthy male Sprague–Dawley (SD) rats (84), SPF grade, weighing 220–240 g, were purchased from Hunan Slake

Jinda Laboratory Animal Co. (Certificate of Conformity No. SCXK [Hunan] 2019-0004). The animal room was clean and ventilated to maintain the appropriate temperature (22–24 °C), with a 12-h light/dark cycle. All animal experiments were approved by the Science and Technology Ethics Committee of Tongji University (approval number: TJBH21324201, 2024.3.1). The experimental procedures followed the National Guidelines for Laboratory Animal Ethics. All rats were euthanized by intraperitoneal injection of an overdose of sodium pentobarbital (160 mg/kg) for tissue collection (Omolaoye and Du Plessis 2021).

SCI model generation

A rat carotid five-unilateral clamp SCI model was prepared using an aneurysm clip (FT228T; B. Braun, Germany) (Li et al. 2019). On the day of surgery, rats were anesthetised with an intraperitoneal injection of sodium pentobarbital (45 mg/kg). The skin, fascia, muscle, and other tissues were separated layer-by-layer according to the anatomical structure. The bony structures, such as the cervical 5 (C5) spinous process and vertebral plate, were removed with bone-biting forceps to fully expose the C5 tissues. An aneurysm clip was slowly inserted from the right side of the C5 spinal cord tissue. When the clip's anterior end reached half the diameter of the spinal cord, it was released, applying pressure for 30 s. The wound was sutured in layers, disinfected with iodine povidone, and the operation was completed. In the sham operation group, the vertebral plate was removed without clamping the spinal cord.

Experimental design

As shown in Fig. 1, rats were acclimated and fed for 1 week before the formal experiments began. Motor functions were assessed 1 day before surgery and 3, 7, 14, and 28 days after. Faeces were collected for gas chromatography-mass spectrometry (GC-MS) 7 days after SCI, and spinal cord tissues were collected 7 and 28 days after surgery for biomolecular experiments.

For Study 1, 12 male SD rats were randomly divided into two groups of six: SCI (surgery) and sham (no surgery). For Study 2, 72 male SD rats were randomly divided into three groups of 24: NaB (SCI surgery + NaB gavage), SCI, and sham. NaB (Sigma, USA) was dissolved in saline and administered by gavage at 300 mg/kg once daily after SCI surgery. The NaB dose was obtained from other disease models (Wang et al. 2011; Park and Sohrabji 2016; Kim and Chuang 2014; Sharma et al. 2015). The SCI and sham groups received equal volumes of saline once daily.

Detection of SCFAs

Samples were extracted in 50 µL of 15% phosphoric acid with 100 µL of 125 µg/mL 4-methylvaleric acid solution as an internal standard and 400 µL ether. Subsequently,

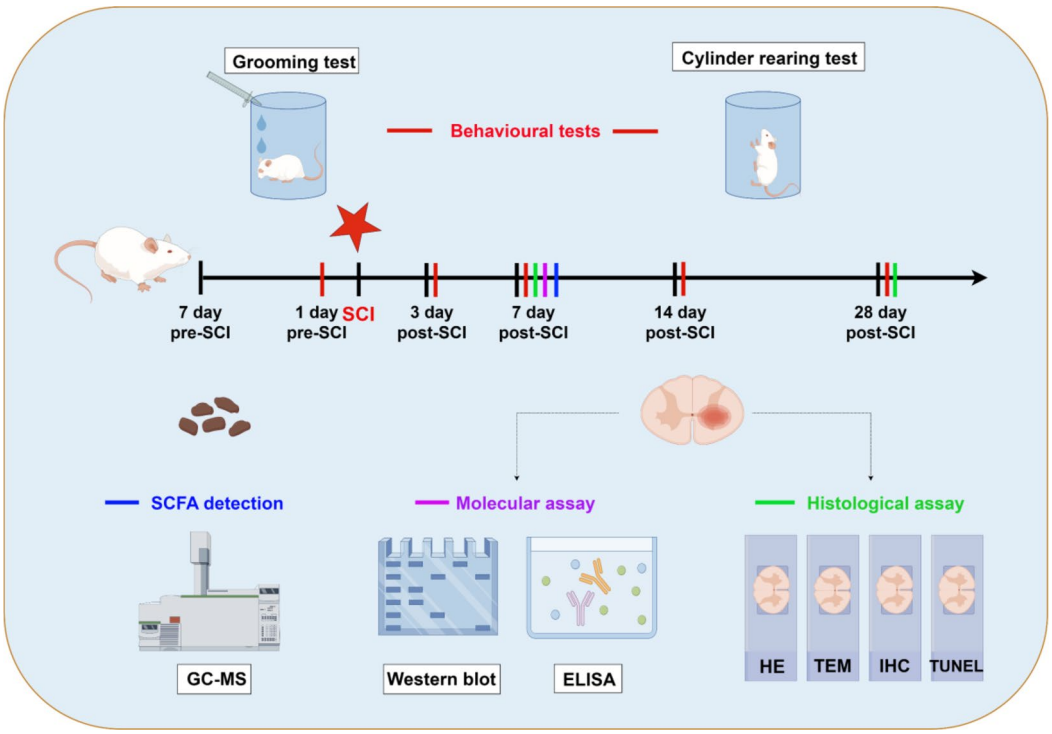

Fig. 1 Schematic of the experimental design and main molecular biological assays at predetermined time points of this study

samples were centrifuged at 4 °C for 10 min at 12 000 rpm after vortexing for 1 min. The supernatant was transferred to a vial for GC-MS analysis. GC was performed using a Trace 1300 gas chromatograph (Thermo Fisher Scientific, USA) with an Agilent HP-INNOWAX capillary column (30 m × 0.25 mm ID × 0.25 μm). Helium was used as the carrier gas at 1 mL/min. Injection was performed in split mode at 10:1 with an injection volume of 1 μL and an injector temperature of 250 °C. The ion source and interface temperatures were 300 °C and 250 °C, respectively. The column temperature was programmed to increase from an initial 90 °C to 120 °C at 10 °C/min, then to 150 °C at 5 °C/min, and finally to 250 °C at 25 °C/min, which was maintained for 2 min (total run-time of 15 min).

Mass spectrometric detection of metabolites was performed on an ISQ 7000 (Thermo Fisher Scientific) in electron impact ionisation mode, using single-ion monitoring mode with an electron energy of 70 eV.

Behavioural tests

Motor function recovery of the affected limb was assessed 1 day before surgery and 3, 7, 14, and 28 days after surgery. The cylinder rearing test is widely used to evaluate forelimb motor deficits in rats (Roome and Vanderluit 2015). The assessor recorded the number of times the affected forelimb touched the cylinder wall and calculated the utilisation rate of the affected limb. The grooming test assesses the motor function of rats by observing the magnitude of the forelimb range of motion (Streijger et al. 2014). The assessor observed the size and range of activity of the affected forelimb during grooming and scored the rats. A score of 0 indicated that the animal could not contact any part of its face or head with its forepaws, and 5 indicated that it could contact the area behind the ears. The results were evaluated by trained researchers who were unaware of the experimental group assignments.

Haematoxylin-eosin staining

On the 28th day after surgery, a 1-cm section of spinal cord tissue centred on the injury site was removed and immediately fixed in 4% paraformaldehyde for 24 h. The experimental procedure was referred to the published literature (Wang et al. 2022; Khodir et al. 2024). The tissue was dehydrated, embedded in paraffin, and sectioned for haematoxylin–eosin (HE) staining. Results were observed under a microscope, and images were saved. The size of the cavity area of the spinal cord tissue was measured using ImageJ software. Assessors were unaware of the experimental group assignments. All these measurements were assessed in three sections for each animal, at three-non overlapping high-power fields of magnification (×100, ×400).

Transmission electron microscopy

Seven days post-surgery, spinal cord tissues were collected and placed in an electron microscope fixative solution for storage and as spare. After fixation for 2 h using 1% osmium solution, dehydration, infiltration, and embedding were performed sequentially. The embedded samples were polymerised in a 60°C oven for 48 h, and the resin block was taken out as spare. A 60–80 nm ultrathin slicer was used for sectioning. The sections were stained with 2% uranyl acetate-saturated alcohol solution to block light, followed by 2.6% lead citrate solution to prevent carbon dioxide staining. The sections were dried overnight at room temperature (Su et al. 2023). Transmission electron microscopy (TEM) was then used to observe cell morphology and intracellular organelles.

Terminal deoxynucleotidyl transferase dUTP nick-end labelling staining

Seven days post-surgery, terminal deoxynucleotidyl transferase dUTP nick-end labelling (TUNEL) staining was performed using a one-step TUNEL Apoptosis In Situ Detection Kit (KeyGEN, China).The prepared spinal cord sections were baked, deparaffinised, and hydrated. Proteinase K working solution, TdT enzyme reaction solution, and fluorescent labelling solution were added sequentially according to the kit instructions, followed by DAPI staining solution to re-stain the nuclei of the cells while avoiding light. Finally, the DAPI staining solution was washed off and sealed with a fluorescent sealer (Wang et al. 2022). Staining was observed under a fluorescence microscope, and images were captured and stored.

Western blot analysis

Seven days post-surgery, spinal cord tissues were collected. The collected spinal cord tissue was divided into two sections to ensure that the center of the injury was evenly distributed between both parts. One section was used for protein extraction and subsequent Western blot analysis, while the other section was used for enzyme-linked immunosorbent assay. Total protein was extracted using a protein extraction kit (Solarbio, China). The experimental procedure was referred to the published literature (Hou et al. 2021a). Protein concentration was determined using the BCA Protein Content Assay Kit (KeyGEN). Separation and concentration gels were prepared according to the ratio; the samples were spiked, electrophoresed, transferred to the membrane

sequentially, and blocked with 5% skim milk for 1 h. Primary antibodies used were NLRP3 (1:1000, bs-24563R, BIOSYNTHESIS), apoptosis-associated speck-like protein (ASC) (1:1000, ab180799, Abcam), Caspase-1 (1:1000, NBP1-45433, Novus), GSDMD (1:1000, EPR20859, Abcam), IL-18 (1:2000, 10663-1-AP, Proteintech), and IL-1β (1:1000, ab254360, Abcam). Membranes were incubated overnight at 4 °C, then with secondary antibodies at room temperature for 1 h. Finally, photos were developed using a gel imaging system, and the grey level of the protein of each band was quantitatively analysed with ImageJ software.

Immunohistochemistry staining

SABC immunohistochemistry kit (Solarbio) was used for immunohistochemistry (IHC) staining, and the prepared sections were baked, deparaffinised, hydrated, and subjected to antigen repair, endogenous peroxidase inactivation, closure, and incubation at 4 °C with primary antibodies NLRP3 (1:1000, bs-24563R, BIOSYNTHESIS), ASC (1:1000, ab180799, Abcam), Caspase-1 (1:1000, NBP1-45433, Novus), and GSDMD (1:1000, EPR20859, Abcam). Secondary antibody incubation at room temperature was followed by a colour development reaction using the DAB working solution, mild haematoxylin counterstaining, dehydration, and sealing. Images were captured using a microscope (Mohammad et al. 2023; Chen et al. 2023). All these measurements were assessed in three sections for each animal, at three-non overlapping high-power fields of magnification (×400).

Enzyme-linked immunosorbent assay

According to the enzyme-linked immunosorbent assay (ELISA) detection kit (RUIXIN, China), standard and sample wells were set up, and the HRP-labelled antibody was added to each well and incubated for 1 h at room temperature, followed by repeated washing and drying. Substrates A and B were added to each well and allowed to react fully. IL-18 and IL-1β concentrations were measured at 450 nm (Ye et al. 2018).

Statistical analysis

Statistical analysis was conducted using IBM-SPSS 26.0. Data are expressed as mean ± standard deviation. Independent sample t-tests were used for comparisons between two independent groups. Comparisons among more than three groups were performed using one-way analysis of variance with LSD (equal variances assumed). $P < 0.05$ was considered statistically significant.

Results

Faecal SCFA levels are altered after SCI

We analysed the SCFAs content in faecal samples from SCI and sham groups rats using GC-MS. The most abundant SCFAs in both groups were acetic, propionic, and butyric acids. Compared to the sham group, the SCI group had significantly lower levels of butyric acid ($P = 0.041$), hexanoic acid ($P = 0.045$), isobutyric acid ($P = 0.039$), isovaleric acid ($P = 0.042$), and propionic acid ($P = 0.040$). Levels of acetic acid ($P = 0.153$) and valeric acid ($P = 0.146$) did not differ significantly between the groups (Fig. 2A and H). These findings indicate significant changes in gut flora metabolites (SCFAs) after SCI.

SCFAs negatively correlate with inflammatory factors IL-18 and IL-1β

SCFAs levels differed between the SCI and sham groups, suggesting that SCFAs serve as potential interventions for SCI treatment. Because IL-18 and IL-1β are key inflammatory factors released during pyroptosis (Rao et al. 2022), we examined their levels in both groups. IL-18 ($P = 0.00095$) and IL-1β ($P = 0.021$) levels were significantly higher in the SCI group compared to those in the sham group (Fig. 3A and B). We performed Pearson correlation analysis to find the SCFAs with the highest correlation with IL-18 and IL-1β (Fig. 3C and M). The results showed that in the SCI group, propionic acid levels were not significantly correlated with IL-1β levels (Fig. 3M) but were negatively correlated with IL-18 levels ($r = -0.856$, $P = 0.030$) (Fig. 3H). Butyric acid levels were negatively correlated with both IL-18 ($r = -0.868$, $P = 0.025$) and IL-1β ($r = -0.841$, $P = 0.036$) levels (Fig. 3D and I). These results indicate that butyric and propionic acids are significantly negatively correlated with key inflammatory factors for pyroptosis after SCI, with butyric acid showing the highest correlation.

NaB attenuates pathological SCI and promotes motor function recovery in SCI rats

To further investigate the effect of butyric acid on rats with SCI, we administered NaB by gavage and assessed motor function recovery using cylinder rearing and grooming tests. One day before SCI, there was no significant difference in the affected limb utilisation rate among the groups. Three days postoperatively, rats in the SCI and NaB groups relied more on their healthy forelimbs for postural support, with a significantly lower utilisation rate of the affected forelimb than the sham group. By 28 days postoperatively, the forelimb utilisation rate was significantly higher in the

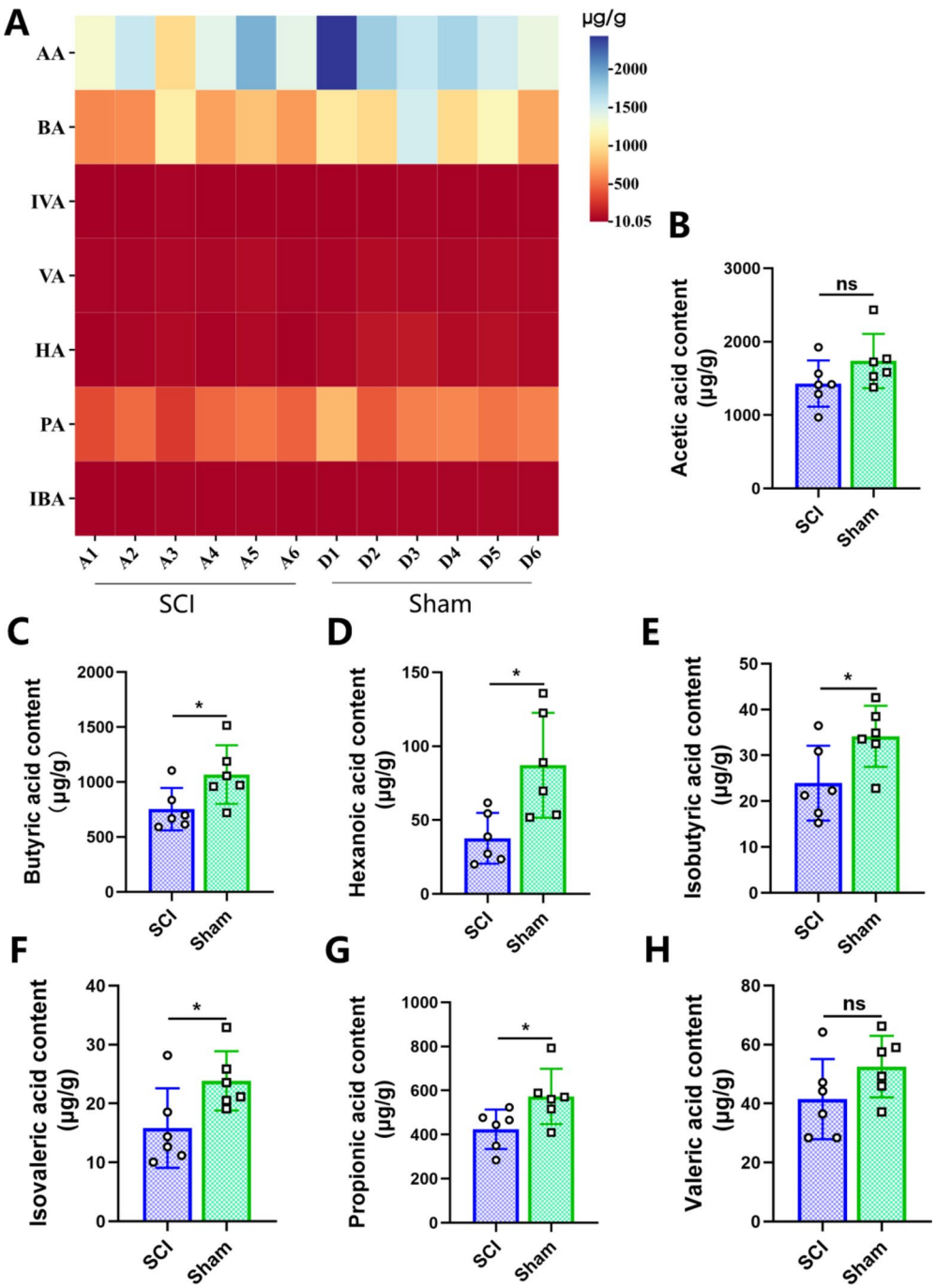

Fig. 2 Changes in faecal short-chain fatty acids (SCFAs) levels after spinal cord injury (SCI). (**A**) Heatmap indicating the levels of SCFAs in the faeces of sham and SCI groups ($n=6$); (**B**) Acetic acid levels in sham and SCI groups ($n=6$); (**C**) Butyric acid levels in sham and SCI groups ($n=6$); (**D**) Hexanoic acid levels in sham and SCI groups ($n=6$); (**E**) Isobutyric acid levels in sham and SCI groups ($n=6$); (**F**) Isovaleric acid levels in sham and SCI groups ($n=6$); (**G**) Propionic acid levels in sham and SCI groups ($n=6$); (**H**) Valeric acid levels in sham and SCI groups ($n=6$). *$P<0.05$ compared to the sham group

NaB group than in the SCI group ($P=0.013$) (Fig. 4A). A similar trend was observed in grooming tests, where scores were significantly higher in the NaB group than in the SCI group at 28 days postoperatively ($P=0.010$) (Fig. 4B). These results suggest that NaB promotes forelimb motor function recovery in rats with SCI.

To clarify the effect of NaB on pathological spinal cord damage, we performed HE staining using paraffin sections of the spinal cord. Compared to the sham group, the SCI group exhibited significant tissue damage, with large cavities, severe vacuolisation, blurred boundaries between white and grey matter, and reduced neuron numbers. In contrast,

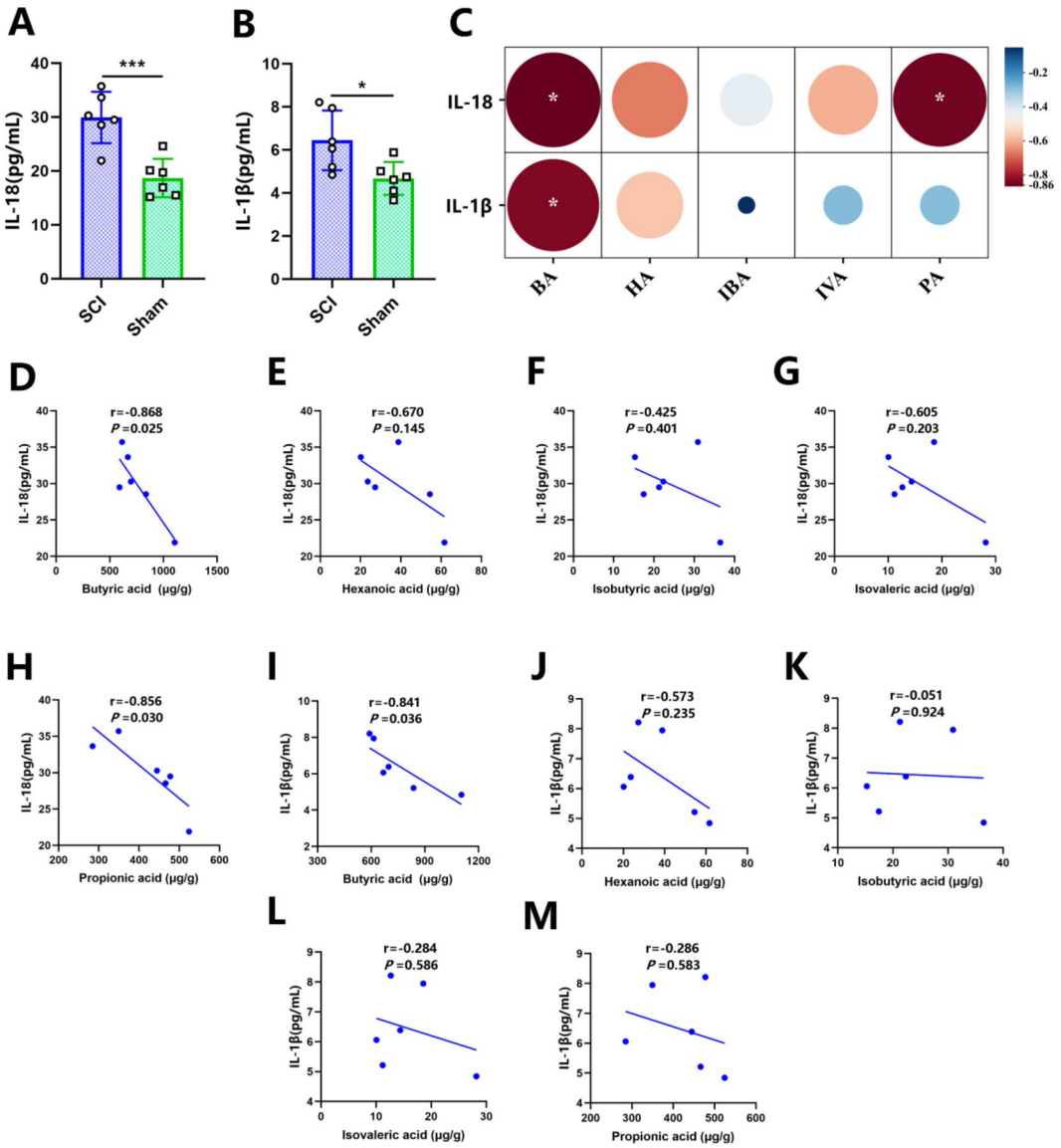

Fig. 3 Correlation analysis of faecal short-chain fatty acids (SCFAs) with inflammatory factors interleukin-18 (IL-18) and interleukin-1β (IL-1β) in spinal cord injury (SCI) rats. (**A**) Levels of inflammatory factor IL-18 in sham and SCI groups ($n=6$); (**B**) Levels of inflammatory factor IL-1β in sham and SCI groups ($n=6$); (**C**) Heatmap analysis of the correlation between SCFAs and inflammatory factors; (**D**) Correlation analysis of butyric acid with IL-18 ($n=6$); (**E**) Correlation analysis of hexanoic acid with IL-18 ($n=6$); (**F**) Correlation analysis of isobutyric acid with IL-18 ($n=6$); (**G**) Correlation analysis of isovaleric acid with IL-18 ($n=6$); (**H**) Correlation analysis of propionic acid with IL-18 ($n=6$); (**I**) Correlation analysis of butyric acid with IL-1β ($n=6$); (**J**) Correlation analysis of hexanoic acid with IL-1β ($n=6$); **K**. Correlation analysis of isobutyric acid with IL-1β ($n=6$); **L**. Correlation analysis of isovaleric acid with IL-1β ($n=6$); **M**. Correlation analysis of propionic acid with IL-1β ($n=6$). $^{*}P<0.05$, $^{**}P<0.01$, $^{***}P<0.001$ compared to the sham group

the NaB group had smaller cavity areas, with reduced vacuolisation and degree of damage (Fig. 4C). Quantifying the cavity area of spinal cord tissues in each group revealed that the NaB group had a significantly lower percentage of cavity area than the SCI group ($P=0.002$) (Fig. 4D). These findings suggest that NaB attenuates pathological spinal cord damage in rats with SCI.

NaB inhibits spinal cord neuronal pyroptosis in SCI rats

To explore the effects of NaB on neuronal pyroptosis in SCI rats, we used TEM to observe the integrity of neuronal cell membranes in each group. Compared to the sham group, the SCI group exhibited swollen nerve cells, localised

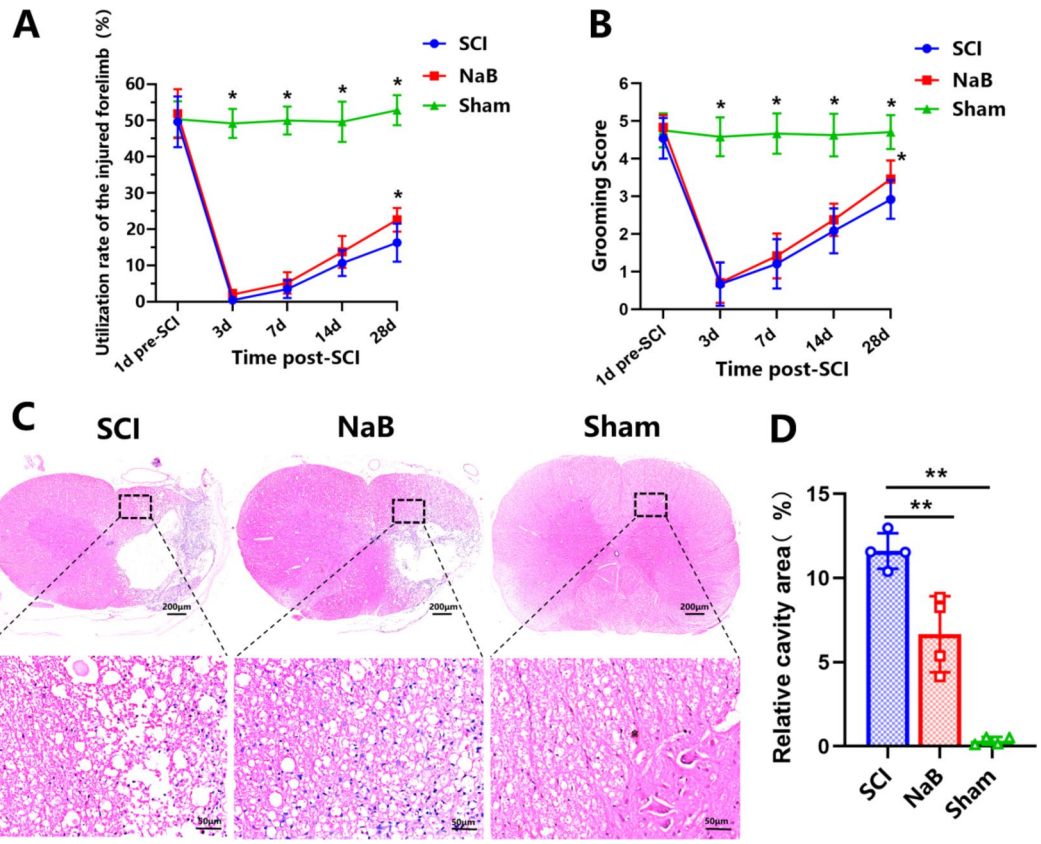

Fig. 4 Sodium butyrate (NaB) attenuates pathological spinal cord injury and promotes motor function recovery in spinal cord injury (SCI) rats. (**A**) Results of the cylinder rearing test for each group of rats at different time points ($n=12$); (**B**) Results of the grooming test for each group of rats at different time points ($n=12$); (**C**) Representative pictures of haematoxylin-eosin (HE) staining of spinal cord cross-sections, with scale bars of 200 μm in the upper panel and 50 μm in the lower panel; (**D**) Percentage of spinal cord cavity area ($n=4$). *$P<0.05$, **$P<0.01$ compared to the SCI group

cell membrane rupture, pores, and the disappearance of mitochondrial cristae and other features of pyroptosis. In contrast, the NaB group had less swollen nerve cells, occasional cell membrane pores, and reduced mitochondrial damage (Fig. 5A). TUNEL staining revealed significantly more TUNEL-positive cells in the SCI group than in the sham group, whereas the NaB group had significantly fewer TUNEL-positive cells than the SCI group ($P=0.023$) (Fig. 5B and C).

Because pyroptosis is accompanied by inflammatory factor release, we used ELISA and WB to detect inflammatory factor levels in the spinal cord. ELISA results indicated that IL-1β and IL-18 levels were significantly higher in the SCI group compared to the sham group but significantly lower in the NaB group than in the SCI group ($P=0.013$ for both IL-1β and IL-18) (Fig. 5D and E). WB results corroborated these findings, showing elevated IL-1β and IL-18 expression in the SCI group, which were significantly reduced in the NaB group (IL-18, $P=0.016$; IL-1β, $P=0.018$) (Fig. 5F and H). These results suggest that NaB effectively reduces SCI neuronal pyroptosis and decreases the inflammatory response.

NaB inhibits activation of the NLRP3 inflammatory vesicle-associated pyroptosis pathway

The NLRP3/Caspase-1/GSDMD pathway is crucial in pyroptosis following SCI (Al Mamun et al. 2021). To explore the effect of NaB on the expression of NLRP3/Caspase-1/GSDMD pathway-related proteins, we examined the expression of key proteins in each group using WB and IHC staining. IHC results showed that the intensity and range of positive staining for the NLRP3, ASC, Caspase-1, and GSDMD proteins were significantly increased in the SCI group compared to the sham group, whereas the NaB group exhibited significantly decreased staining compared to the SCI group (Fig. 6E).

The mean optical density values for NLRP3, ASC, Caspase-1, and GSDMD were significantly higher in the SCI group than in the sham group, and the mean optical density

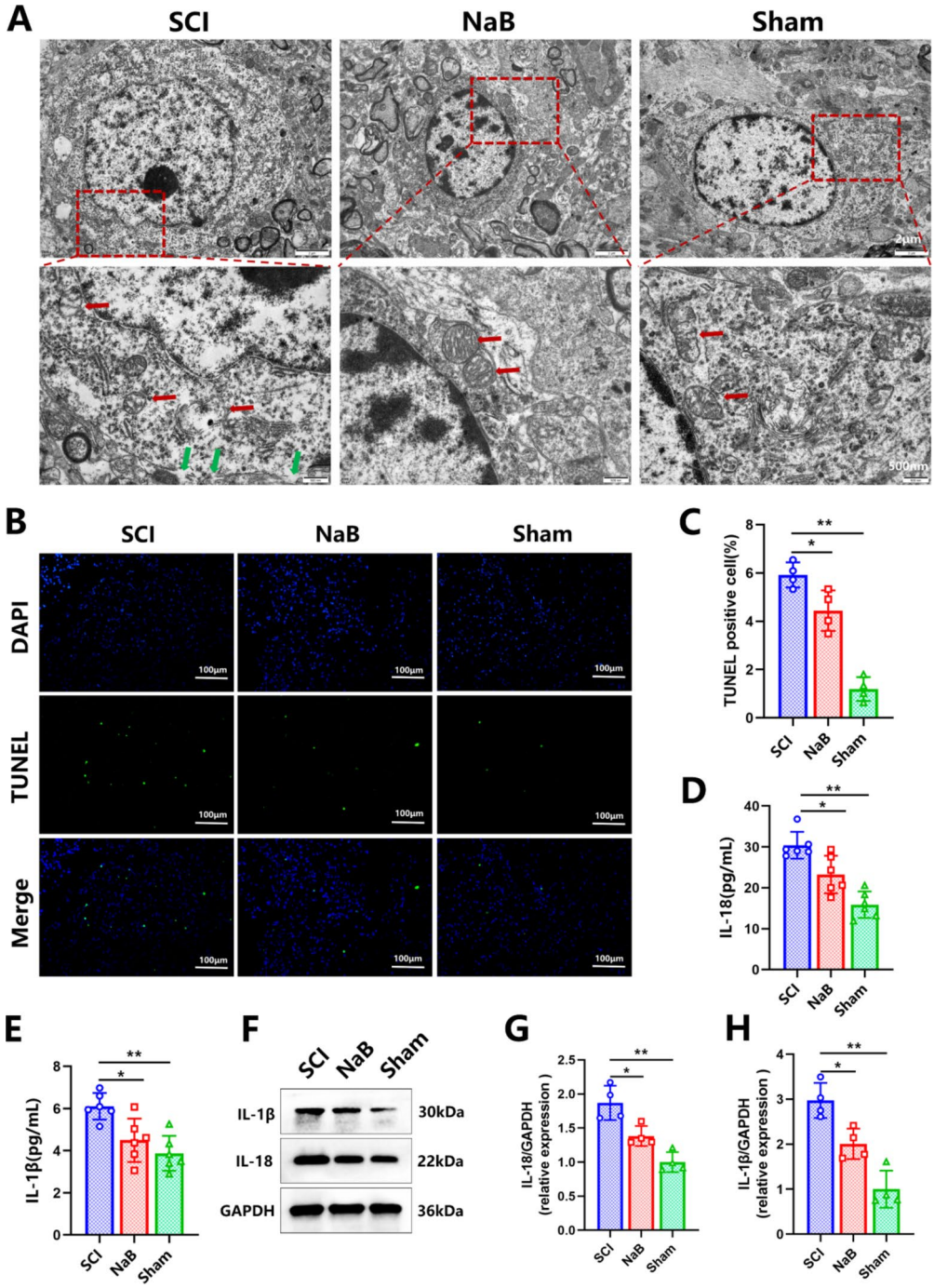

Fig. 5 Sodium butyrate (NaB) inhibits pyroptosis and attenuates inflammatory response in spinal cord injury (SCI) rats. (**A**) Representative transmission electron microscopy (TEM) images of the spinal cord for each group. Red arrows indicate mitochondria and green arrows indicate cell membrane pores. Scale bar is 2 μm in the upper image and 500 nm in the lower image; (**B**) Representative terminal deoxynucleotidyl transferase dUTP nick-end labelling (TUNEL) staining images for each group, scale bar is 100 μm; (**C**) Quantitative analysis of TUNEL-positive cells ($n=4$); (**D**) Levels of inflammatory factor IL-18 detected by enzyme-linked immunosorbent assay (ELISA) ($n=4$); (**E**) Levels of inflammatory factor IL-1β detected by ELISA ($n=4$); (**F**) Representative western blot (WB) strips for inflammatory factors IL-18 and IL-1β; (**G**) Levels of inflammatory factor IL-18 measured by WB ($n=4$); (**H**) Levels of inflammatory factor IL-1β measured by WB ($n=4$). *$P<0.05$, **$P<0.01$ compared with the SCI group

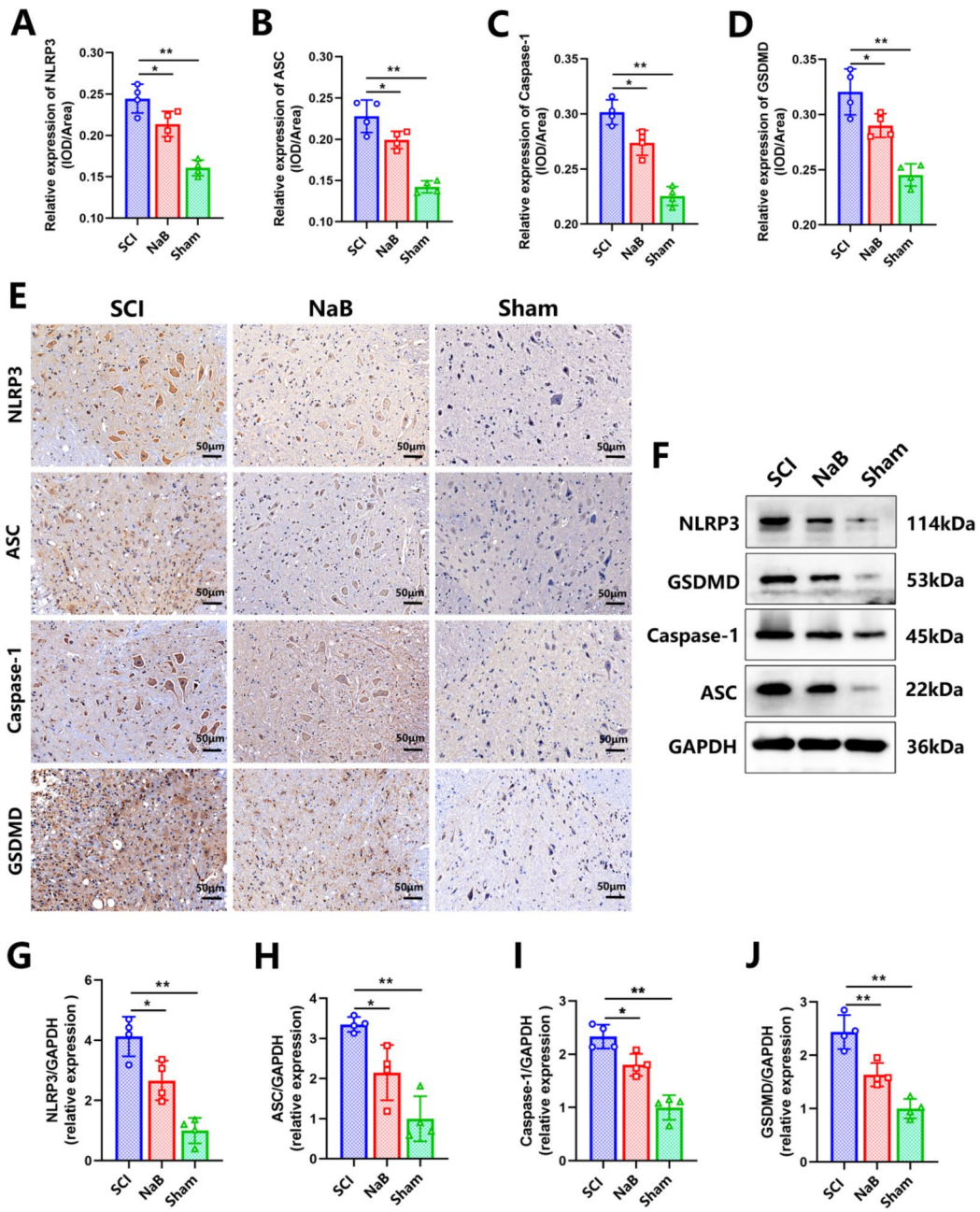

Fig. 6 Sodium butyrate (NaB) inhibits the expression of the NOD-like receptor protein 3 (NLRP3)/cysteinyl aspartate specific proteinase 1 (Caspase-1)/gasdermin D (GSDMD) pyroptosis pathway. (**A**) Mean optical density values of NLRP3 in each group ($n=4$); (**B**) Mean optical density values of apoptosis-associated speck-like protein containing a CARD (ASC) in each group ($n=4$); (**C**) Mean optical density values of Caspase-1 in each group ($n=4$); (**D**) Mean optical density values of GSDMD in each group ($n=4$); (**E**) Representative images of immunohistochemistry (IHC) staining for key proteins involved in pyroptosis; (**F**) Representative western blot (WB) bands for key pyroptosis proteins; (**G**) Expression levels of NLRP3 in each group ($n=4$); (**H**) Expression levels of ASC in each group ($n=4$); (**I**) Expression levels of Caspase-1 in each group ($n=4$); (**J**) Expression levels of GSDMD in each group ($n=4$). $^{*}P<0.05$ and $^{**}P<0.01$ compared with the SCI group

values of NLRP3 ($P=0.036$), ASC ($P=0.036$), Caspase-1 ($P=0.011$), and GSDMD ($P=0.040$) were significantly lower in the NaB group than in the SCI group (Fig. 6A and D). WB results confirmed that expression levels of these proteins were significantly higher in the SCI group than in the sham group but markedly lower in the NaB group; NLRP3 ($P=0.017$), ASC ($P=0.025$), Caspase-1 ($P=0.020$), and GSDMD ($P=0.003$) (Fig. 6F and J). These results suggest that NaB reduces the expression of NLRP3/Caspase-1/GSDMD pyroptosis pathway-related proteins.

Discussion

Recent evidence indicates that SCFAs are significantly reduced in patients with SCI, and supplementation with SCFAs promotes motor function recovery in SCI mice (Jing et al. 2023). SCFAs are produced by anaerobic bacterial fermentation of indigestible carbohydrates, including acetic, propionic, butyric, isobutyric, isovaleric, valeric, and hexanoic acids (He et al. 2024). SCFAs have many beneficial properties mediated through immune, vagal, endocrine, or humoral pathways that affect gut–brain communication and brain function (Dalile et al. 2019; Koh et al. 2016). In the central nervous system, SCFAs influence neuroinflammation by affecting glial cell morphology and function, modulating neurotrophic factors, increasing neurogenesis, contributing to serotonin biosynthesis, and improving neuronal homeostasis and function (Silva et al. 2020). Jing et al. (2021) examined SCFA concentrations in the faeces of an SCI mouse model, showing that butyric acid was reduced by 58.6%, propionic acid by 21.2%, isobutyric acid by 39.4%, and caproic acid by 31.8% in the SCI group compared to the sham group. A clinical observational study also found that acetic, propionic, and butyric acids were significantly downregulated in patients with SCI compared to healthy participants (Jing et al. 2023).

Our findings revealed significant reductions in butyric, caproic, isobutyric, isovaleric, and propionic acid levels and significant changes in SCFA levels after SCI. We assessed the correlation between these SCFAs and key inflammatory factors (IL-18 and IL-1β) for pyroptosis. The results indicate that reduced faecal levels of SCFAs (butyric acid and propionic acid) correlate with elevated inflammatory factors in the spinal cord of SCI rats, with butyric acid showing the highest correlation. Lanza et al. (2019) found that NaB intervention significantly ameliorated histopathological changes in SCI mice, promoted motor function recovery, and modulated the NF-κB pathway, significantly reducing inflammatory factor expression. This evidence suggests that butyric acid may be a potential intervention for promoting SCI recovery.

Butyric acid production depends on diet composition and intestinal flora (Fu et al. 2019). NaB is a common butyric acid compound, and its beneficial effects have been extensively studied (Bourassa et al. 2016). In recent years, many studies have confirmed that NaB has a neuroprotective role in various neurological disorders, such as stroke (Patnala et al. 2017; Sun et al. 2015; Zhou et al. 2021), Parkinson's (Hou et al. 2021b), epilepsy (Li et al. 2021), and traumatic brain injury (Li et al. 2016), improving neurological deficits. Sharma et al. (Sharma et al. 2015) evaluated NaB in a rat model of Parkinson's, showing that rats in the NaB group outperformed the model group in the narrow beam walking test, rotating rod test, and spontaneous locomotion, suggesting that NaB significantly restores motor and coordination abilities in rats with Parkinson's. Guo et al.(Guo et al. 2023) found that NaB improved motor function, increased striatal neurotransmitter levels, reduced dopaminergic neuron death, and restored disturbed gut microbiota in Parkinson's mice. In a mouse model of seizures, brain injury and neurological deficits can be attenuated by treatment with NaB through the activation of Nrf2 pathway and the improvement of mitochondrial function (Li et al. 2021). Park et al. (Park and Sohrabji 2016) found that NaB attenuated sensorimotor deficits, attenuated inflammation and oxidative stress injury, and promoted motor function recovery in female stroke rats. He et al. (He et al. 2022) demonstrated that NaB treatment improved pathological damage in the cerebral cortex and hippocampus of cerebral ischemia-hypoxic neonatal rats, significantly reducing neuronal atrophy and nuclear chromatin condensation. In a mouse model of traumatic brain injury, NaB significantly improved brain histopathological changes, reduced neuronal damage, and attenuated neurological deficits, cerebral oedema, and blood–brain barrier damage (Li et al. 2016).

The results of the present study align with those described above: 28 days after SCI modelling, rats in the NaB group had significantly higher scores in the cylinder rearing and grooming tests compared to the SCI group. In addition, HE staining revealed less spinal cord tissue damage and a lower percentage of cavity area in the NaB group than in the SCI group. These results suggest that NaB plays a neuroprotective role in SCI by reducing pathological damage to the spinal cord and promoting motor function recovery.

Studies have shown that butyric acid possesses anti-inflammatory, antioxidant, and anti-apoptotic properties (Berni Canani et al. 2012) and is associated with energy homeostasis, immune system regulation, and brain function (Stilling et al. 2016). Gu et al. (Gu et al. 2019) found that NaB significantly inhibits glomerular endothelial cell pyroptosis and reduces IL-1β and IL-18 levels, thereby decreasing inflammation. Zhang et al. (2021) discovered that NaB ameliorates hepatic steatosis in mice by inhibiting pyroptosis and inflammation. WANG et al. (Wang et al. 2019) demonstrated that NaB significantly attenuated neurological deficits, improved neuronal survival, reduced the levels of inflammatory factors such as IL-1β, TNF-α and IL-8, and decreased the expression of TUNEL-positive cells in mice with cerebral ischemia/reperfusion injury.

Our TEM results showed that NaB reduced neuronal cell swelling with occasional cell membrane pores and reduced mitochondrial damage. TUNEL staining is commonly used to detect DNA damage in apoptotic cells. DNA damage also occurs during pyroptosis, and studies have shown that the TUNEL assay is positive during pyroptosis (Yang et al.

2020). Our TUNEL staining revealed a significantly lower rate of DNA damage in the NaB group compared to the SCI group. ELISA and WB showed decreased IL-1β and IL-18 levels in rats in the NaB group compared to the SCI group. In addition, our study demonstrated that NaB reduced the expression of the pyroptosis execution protein GSDMD in rats following SCI. These findings suggest that NaB effectively inhibits neuronal pyroptosis and reduces the inflammatory response following SCI in rats.

The classical manifestations of pyroptosis include morphological features such as swollen cell volume, deformed and enlarged mitochondria, DNA degradation, and 10–16 nm pores in the cell membrane. Pro-inflammatory cytokines IL-1β and IL-18 are also released from the cytoplasm during this process (Lu et al. 2020). The essence of pyroptosis is the formation of pores in the cell membrane by gasdermin family proteins, the activation of which can be categorised into a typical pathway mediated by Caspase-1 and an atypical pathway mediated by Caspase-4/5/11 (Al Mamun et al. 2021). Inflammatory vesicles are crucial during pyroptosis; NLRP3 inflammatory vesicles are most closely related to pyroptosis (Broz and Dixit 2016). During the secondary phase of SCI, large amounts of damage-associated molecular patterns and pathogen-associated molecular patterns are released locally and systemically due to injury, triggering downstream inflammatory pathways (Yin et al. 2022). Subsequently, NLRP3, as a pattern recognition receptor, is activated in response to this abnormal stimuli (Sharma and Kanneganti 2016), and the expression of inflammatory vesicle-associated genes such as *NLRP3*, *IL-18*, and *IL-1β* precursors is significantly increased (Kelley et al. 2019). However, NLRP3 will indirectly bind pro-Caspase-1 via ASC, leading to Caspase-1 activation. This promotes the maturation and secretion of IL-1β and IL-18 precursors, as well as GSDMD hydrolysis to form cell membrane pores, thereby triggering intense inflammatory responses and ultimately, pyroptosis (Sharma and de Alba 2021).

NaB has been shown to reduce pyroptosis by inhibiting the Caspase-1/GSDMD pathway, which in turn ameliorates glomerular endothelial cell injury (Gu et al. 2019). NaB also ameliorates alcoholic fatty liver disease by inhibiting GSDMD-mediated pyroptosis (Zhang et al. 2021). Bian et al. (Bian et al. 2023) explored the effects of NaB on mice with colitis and its relationship with molecular mechanisms and found that NaB reduces colitis severity, inhibits NLRP3 inflammatory vesicle activation and NF-κB phosphorylation, and reduces corresponding inflammatory factor levels. Our study demonstrated that NaB decreases NLRP3, ASC, Caspase-1, and GSDMD expression in rats after SCI, suggesting that NaB inhibits the NLRP3/Caspase-1/GSDMD pyroptosis pathway activation.

Despite our promising results, this study had some limitations. First, our study was limited to animal experiments without cellular experiments to further validate specific cell types that undergo pyroptosis. Second, this study only preliminarily explored the effect of NaB on the classical NLRP3/Caspase-1/GSDMD pyroptosis pathway, thereby necessitating the exploration of the role and mechanism of NaB in the non-classical pyroptosis pathway in future research. In addition, although the neuroprotective effects of NaB have been extensively demonstrated in animal models, clinical evidence supporting its neurological benefits in humans remains limited. Reassuringly, oral encapsulated sodium butyrate supplementation has been shown to have a favorable safety profile in humans and may alleviate clinical symptoms in patients with irritable bowel syndrome (Banasiewicz et al. 2013), inflammatory bowel disease (Di Sabatino et al. 2005), and diverticulitis (Krokowicz et al. 2014), but the optimal dose and route of administration need to be further investigated.

Conclusion

Our results showed that SCFAs levels changed significantly after SCI, with butyric acid showing the strongest correlation with inflammatory factor levels in the spinal cord. Additionally, NaB supplementation promoted motor function recovery in rats with SCI, attenuated pathological injury, reduced the expression of NLRP3/Caspase-1/GSDMD pyroptosis pathway proteins, and inhibited neuronal pyroptosis, thus attenuating the inflammatory response. Our findings suggest that butyric acid from the microbiota may effectively promote SCI recovery.

Supplementary Information The online version contains supplementary material available at https://doi.org/10.1007/s11011-025-01589-8.

Acknowledgements We would like to thank Editage (www.editage.cn) for English language editing. We also thank Suzhou Panomike Biomedical Technology for conducting the short-chain fatty acid assay.

Author contributions A. Z., R.P., and J. W. conceived and designed the study. Y. C., Q. C., and J. F. performed the experiments and analysed the data. Y. C. and J. W. wrote the original draft. J.W., L. W., and C. C. collected the samples and performed the experiments. All the authors have read and approved the manuscript for publication.

Funding This work was supported by a grant from the Hongkou District health committee project (HONGWEI-2403-05), the Tongji University Affiliated Shanghai Fourth People's Hospital Research Launch Special Fund (SYKYQD02001), and the Tongji University Affiliated Shanghai Fourth People's Hospital Talent Promotion Program Project (SY-XKZT-2023-1006, SY-XKZT-2023-1013).

Data availability No datasets were generated or analysed during the current study.

Declarations

Ethics approval The animal study protocol was approved by the Science and Technology Ethics Committee of Tongji University. Experimental procedures followed the Chinese National Ethical Principles for Laboratory Animals and relevant regulations of the Animal Ethics Committee at the Fourth People's Hospital Affiliated with Tongji University (approval number: TJBH21324201,2024.3.1).

Consent to participate Not applicable.

Consent to publish Not applicable.

Competing interests The authors declare no competing interests.

References

Al Mamun A, Wu Y, Monalisa I, Jia C, Zhou K, Munir F, Xiao J (2021) Role of pyroptosis in spinal cord injury and its therapeutic implications. J Adv Res 28:97–109

Anjum A, Yazid MD, Fauzi Daud M, Idris J, Ng AMH, Selvi Naicker A, Ismail OHR, Athi Kumar RK, Lokanathan Y (2020) Spinal cord injury: pathophysiology, multimolecular interactions, and underlying recovery mechanisms. Int J Mol Sci 21:7533

Banasiewicz T, Krokowicz Ł, Stojcev Z, Kaczmarek BF, Kaczmarek E, Maik J, Marciniak R, Krokowicz P, Walkowiak J, Drews M (2013) Microencapsulated sodium butyrate reduces the frequency of abdominal pain in patients with irritable bowel syndrome. Colorectal Dis 15:204–209

Bazzocchi G, Turroni S, Bulzamini MC, D'Amico F, Bava A, Castiglioni M, Cagnetta V, Losavio E, Cazzaniga M, Terenghi L, De Palma L, Frasca G, Aiachini B, Cremascoli S, Massone A, Oggerino C, Onesta MP, Rapisarda L, Pagliacci MC, Biscotto S, Scarazzato M, Giovannini T, Balloni M, Candela M, Brigidi P, Kiekens C (2021) Changes in gut microbiota in the acute phase after spinal cord injury correlate with severity of the lesion. Sci Rep 11:12743

Berni Canani R, Di Costanzo M, Leone L (2012) The epigenetic effects of butyrate: potential therapeutic implications for clinical practice. Clin Epigenetics 4:4

Bian Z, Zhang Q, Qin Y, Sun X, Liu L, Liu H, Mao L, Yan Y, Liao W, Zha L, Sun S (2023) Sodium butyrate inhibits oxidative stress and NF-κB/NLRP3 activation in dextran sulfate sodium Salt-Induced colitis in mice with involvement of the Nrf2 signaling pathway and mitophagy. Dig Dis Sci

Bourassa MW, Alim I, Bultman SJ, Ratan RR (2016) Butyrate, neuroepigenetics and the gut microbiome: can a high fiber diet improve brain health? Neurosci Lett 625:56–63

Broz P, Dixit VM (2016) Inflammasomes: mechanism of assembly, regulation and signalling. Nat Rev Immunol 16:407–420

Chen Y, Liu Y, Jiang K, Wen Z, Cao X, Wu S (2023) Linear ubiquitination of LKB1 activates AMPK pathway to inhibit NLRP3 inflammasome response and reduce chondrocyte pyroptosis in osteoarthritis. J Orthop Translat 39:1–11

Chio JCT, Xu KJ, Popovich P, David S, Fehlings MG (2021) Neuroimmunological therapies for treating spinal cord injury: evidence and future perspectives. Exp Neurol 341:113704

Courtine G, Sofroniew MV (2019) Spinal cord repair: advances in biology and technology. Nat Med 25:898–908

Dalile B, Van Oudenhove L, Vervliet B, Verbeke K (2019) The role of short-chain fatty acids in microbiota-gut-brain communication. Nat Rev Gastroenterol Hepatol 16:461–478

Di Sabatino A, Morera R, Ciccocioppo R, Cazzola P, Gotti S, Tinozzi FP, Tinozzi S, Corazza GR (2005) Oral butyrate for mildly to moderately active Crohn's disease. Aliment Pharmacol Ther 22:789–794

Fu X, Liu Z, Zhu C, Mou H, Kong Q (2019) Nondigestible carbohydrates, butyrate, and butyrate-producing bacteria. Crit Rev Food Sci Nutr 59:S130–s152

Gong F, Ge T, Liu J, Xiao J, Wu X, Wang H, Zhu Y, Xia D, Hu B (2022) Trehalose inhibits ferroptosis via NRF2/HO-1 pathway and promotes functional recovery in mice with spinal cord injury. Aging 14:3216–3232

Gu J, Huang W, Zhang W, Zhao T, Gao C, Gan W, Rao M, Chen Q, Guo M, Xu Y, Xu YH (2019) Sodium butyrate alleviates high-glucose-induced renal glomerular endothelial cells damage via inhibiting pyroptosis. Int Immunopharmacol 75:105832

Guo TT, Zhang Z, Sun Y, Zhu RY, Wang FX, Ma LJ, Jiang L, Liu HD (2023) Neuroprotective effects of sodium butyrate by restoring gut microbiota and inhibiting TLR4 signaling in mice with MPTP-induced Parkinson's disease. Nutrients 15:930

He X, Zhang T, Zeng Y, Pei P, Liu Y, Jia W, Zhao H, Bi M, Wang S (2022) Sodium butyrate mediates histone crotonylation and alleviated neonatal rats hypoxic-ischemic brain injury through gut-brain axis. Front Microbiol 13:993146

He M, Wei W, Zhang Y, Xiang Z, Peng D, Kasimumali A, Rong S (2024) Gut microbial metabolites SCFAs and chronic kidney disease. J Transl Med 22:172

Hou J, Lei Z, Cui L, Hou Y, Yang L, An R, Wang Q, Li S, Zhang H, Zhang L (2021a) Polystyrene microplastics lead to pyroptosis and apoptosis of ovarian granulosa cells via NLRP3/Caspase-1 signaling pathway in rats. Ecotoxicol Environ Saf 212:112012

Hou Y, Li X, Liu C, Zhang M, Zhang X, Ge S, Zhao L (2021b) Neuroprotective effects of short-chain fatty acids in MPTP induced mice model of Parkinson's disease. Exp Gerontol 150:111376

Hu X, Chen H, Xu H, Wu Y, Wu C, Jia C, Li Y, Sheng S, Xu C, Xu H, Ni W, Zhou K (2020) Role of pyroptosis in traumatic brain and spinal cord injuries. Int J Biol Sci 16:2042–2050

Huang J, Chen P, Xiang Y, Liang Q, Wu T, Liu J, Zeng Y, Zeng H, Liang X, Zhou C (2022) Gut microbiota dysbiosis-derived macrophage pyroptosis causes polycystic ovary syndrome via steroidogenesis disturbance and apoptosis of granulosa cells. Int Immunopharmacol 107:108717

Huang Y, Wang Z, Ye B, Ma JH, Ji S, Sheng W, Ye S, Ou Y, Peng Y, Yang X, Chen J, Tang S (2023) Sodium butyrate ameliorates diabetic retinopathy in mice via the regulation of gut microbiota and related short-chain fatty acids. J Transl Med 21:451

Jing Y, Yu Y, Bai F, Wang L, Yang D, Zhang C, Qin C, Yang M, Zhang D, Zhu Y, Li J, Chen Z (2021) Effect of fecal microbiota transplantation on neurological restoration in a spinal cord injury mouse model: involvement of brain-gut axis. Microbiome 9:59

Jing Y, Yang D, Bai F, Wang Q, Zhang C, Yan Y, Li Z, Li Y, Chen Z, Li J, Yu Y (2023) Spinal cord injury-induced gut dysbiosis influences neurological recovery partly through short-chain fatty acids. NPJ Biofilms Microbiomes 9:99

Kelley N, Jeltema D, Duan Y, He Y (2019) The NLRP3 inflammasome: an overview of mechanisms of activation and regulation. Int J Mol Sci 20:3328

Khodir SA, Imbaby S, Abdel Allem Amer MS, Atwa MM, Ashour FA, Elbaz AA (2024) Effect of mesenchymal stem cells and melatonin on experimentally induced peripheral nerve injury in rats. Biomed Pharmacother 177:117015

Kigerl KA, Hall JC, Wang L, Mo X, Yu Z, Popovich PG (2016) Gut dysbiosis impairs recovery after spinal cord injury. J Exp Med 213:2603–2620

Kim HJ, Chuang DM (2014) HDAC inhibitors mitigate ischemia-induced oligodendrocyte damage: potential roles of oligodendrogenesis, VEGF, and anti-inflammation. Am J Transl Res 6:206–223

Koh A, De Vadder F, Kovatcheva-Datchary P, Bäckhed F (2016) From dietary fiber to host physiology: Short-Chain fatty acids as key bacterial metabolites. Cell 165:1332–1345

Krokowicz L, Stojcev Z, Kaczmarek BF, Kociemba W, Kaczmarek E, Walkowiak J, Krokowicz P, Drews M, Banasiewicz T (2014) Microencapsulated sodium butyrate administered to patients with diverticulosis decreases incidence of diverticulitis–a prospective randomized study. Int J Colorectal Dis 29:387–393

Lanza M, Campolo M, Casili G, Filippone A, Paterniti I, Cuzzocrea S, Esposito E (2019) Sodium butyrate exerts neuroprotective effects in spinal cord injury. Mol Neurobiol 56:3937–3947

Li H, Sun J, Wang F, Ding G, Chen W, Fang R, Yao Y, Pang M, Lu ZQ, Liu J (2016) Sodium butyrate exerts neuroprotective effects by restoring the blood-brain barrier in traumatic brain injury mice. Brain Res 1642:70–78

Li XG, Du JH, Lu Y, Lin XJ (2019) Neuroprotective effects of Rapamycin on spinal cord injury in rats by increasing autophagy and Akt signaling. Neural Regen Res 14:721–727

Li D, Bai X, Jiang Y, Cheng Y (2021) Butyrate alleviates PTZ-induced mitochondrial dysfunction, oxidative stress and neuron apoptosis in mice via Keap1/Nrf2/HO-1 pathway. Brain Res Bull 168:25–35

Liu X, Zhang Y, Wang Y, Qian T (2021a) Inflammatory response to spinal cord injury and its treatment. World Neurosurg 155:19–31

Liu Z, Yao X, Sun B, Jiang W, Liao C, Dai X, Chen Y, Chen J, Ding R (2021b) Pretreatment with Kaempferol attenuates microglia-mediate neuroinflammation by inhibiting MAPKs-NF-κB signaling pathway and pyroptosis after secondary spinal cord injury. Free Radic Biol Med 168:142–154

Lu F, Lan Z, Xin Z, He C, Guo Z, Xia X, Hu T (2020) Emerging insights into molecular mechanisms underlying pyroptosis and functions of inflammasomes in diseases. J Cell Physiol 235:3207–3221

Mohammad HMF, El-Baz AA, Mahmoud OM, Khalil S, Atta R, Imbaby S (2023) Protective effects of evening primrose oil on behavioral activities, nigral microglia and histopathological changes in a rat model of rotenone-induced parkinsonism. J Chem Neuroanat 127:102206

Omolaoye TS, Du Plessis SS (2021) The effect of streptozotocin induced diabetes on sperm function: a closer look at ages, rages, MAPKs and activation of the apoptotic pathway. Toxicol Res 37:35–46

Pang R, Wang J, Xiong Y, Liu J, Ma X, Gou X, He X, Cheng C, Wang W, Zheng J, Sun M, Bai X, Bai L, Zhang A (2022) Relationship between gut microbiota and lymphocyte subsets in Chinese Han patients with spinal cord injury. Front Microbiol 13:986480

Park MJ, Sohrabji F (2016) The histone deacetylase inhibitor, sodium butyrate, exhibits neuroprotective effects for ischemic stroke in middle-aged female rats. J Neuroinflammation 13:300

Patnala R, Arumugam TV, Gupta N, Dheen ST (2017) HDAC inhibitor sodium Butyrate-Mediated epigenetic regulation enhances neuroprotective function of microglia during ischemic stroke. Mol Neurobiol 54:6391–6411

Rao Z, Zhu Y, Yang P, Chen Z, Xia Y, Qiao C, Liu W, Deng H, Li J, Ning P, Wang Z (2022) Pyroptosis in inflammatory diseases and cancer. Theranostics 12:4310–4329

Roome RB, Vanderluit JL (2015) Paw-dragging: a novel, sensitive analysis of the mouse cylinder test. J Vis Exp (98):e52701

Rowland JW, Hawryluk GW, Kwon B, Fehlings MG (2008) Current status of acute spinal cord injury pathophysiology and emerging therapies: promise on the horizon. Neurosurg Focus 25:E2

Sadler R, Cramer JV, Heindl S, Kostidis S, Betz D, Zuurbier KR, Northoff BH, Heijink M, Goldberg MP, Plautz EJ, Roth S, Malik R, Dichgans M, Holdt LM, Benakis C, Giera M, Stowe AM, Liesz A (2020) Short-Chain fatty acids improve poststroke recovery via immunological mechanisms. J Neurosci 40:1162–1173

Sharma M, de Alba E (2021) Structure, activation and regulation of NLRP3 and AIM2 inflammasomes. Int J Mol Sci 22:872

Sharma D, Kanneganti TD (2016) The cell biology of inflammasomes: mechanisms of inflammasome activation and regulation. J Cell Biol 213:617–629

Sharma S, Taliyan R, Singh S (2015) Beneficial effects of sodium butyrate in 6-OHDA induced neurotoxicity and behavioral abnormalities: modulation of histone deacetylase activity. Behav Brain Res 291:306–314

Silva YP, Bernardi A, Frozza RL (2020) The role of Short-Chain fatty acids from gut microbiota in gut-Brain communication. Front Endocrinol (Lausanne) 11:25

Song YH, Agrawal NK, Griffin JM, Schmidt CE (2019) Recent advances in nanotherapeutic strategies for spinal cord injury repair. Adv Drug Deliv Rev 148:38–59

Stilling RM, van de Wouw M, Clarke G, Stanton C, Dinan TG, Cryan JF (2016) The neuropharmacology of butyrate: the bread and butter of the microbiota-gut-brain axis? Neurochem Int 99:110–132

Streijger F, Lee JH, Duncan GJ, Ng MT, Assinck P, Bhatnagar T, Plunet WT, Tetzlaff W, Kwon BK (2014) Combinatorial treatment of acute spinal cord injury with Ghrelin, ibuprofen, C16, and ketogenic diet does not result in improved histologic or functional outcome. J Neurosci Res 92:870–883

Su P, Mao X, Ma J, Huang L, Yu L, Tang S, Zhuang M, Lu Z, Osafo KS, Ren Y, Wang X, Lin X, Huang L, Huang X, Braicu EI, Sehouli J, Sun P (2023) ERRα promotes glycolytic metabolism and targets the NLRP3/caspase-1/GSDMD pathway to regulate pyroptosis in endometrial cancer. J Exp Clin Cancer Res 42:274

Sun J, Wang F, Li H, Zhang H, Jin J, Chen W, Pang M, Yu J, He Y, Liu J, Liu C (2015) Neuroprotective effect of sodium butyrate against cerebral ischemia/reperfusion injury in mice. Biomed Res Int 2015:395895

Wang Z, Leng Y, Tsai LK, Leeds P, Chuang DM (2011) Valproic acid attenuates blood-brain barrier disruption in a rat model of transient focal cerebral ischemia: the roles of HDAC and MMP-9 Inhibition. J Cereb Blood Flow Metab 31:52–57

Wang RX, Li S, Sui X (2019) Sodium butyrate relieves cerebral ischemia-reperfusion injury in mice by inhibiting JNK/STAT pathway. Eur Rev Med Pharmacol Sci 23:1762–1769

Wang YW, Dong HZ, Tan YX, Bao X, Su YM, Li X, Jiang F, Liang J, Huang ZC, Ren YL, Xu YL, Su Q (2022) HIF-1α-regulated lncRNA-TUG1 promotes mitochondrial dysfunction and pyroptosis by directly binding to FUS in myocardial infarction. Cell Death Discov 8:178

Wu D, Wang S, Yu G, Chen X (2021) Cell death mediated by the pyroptosis pathway with the aid of nanotechnology: prospects for cancer therapy. Angew Chem Int Ed Engl 60:8018–8034

Yang Y, Liu PY, Bao W, Chen SJ, Wu FS, Zhu PY (2020) Hydrogen inhibits endometrial cancer growth via a ROS/NLRP3/caspase-1/GSDMD-mediated pyroptotic pathway. BMC Cancer 20:28

Ye Z, Liang Y, Ma Y, Lin B, Cao L, Wang B, Zhang Z, Yu H, Li J, Huang M, Zhou K, Zhang Q, Liu X, Zeng J (2018) Targeted photodynamic therapy of cancer using a novel gallium (III) Tris (ethoxycarbonyl) corrole conjugated-mAb directed against cancer/testis antigens 83. Cancer Med 7:3057–3065

Yin J, Gong G, Wan W, Liu X (2022) Pyroptosis in spinal cord injury. Front Cell Neurosci 16:949939

Zhang T, Li J, Liu CP, Guo M, Gao CL, Zhou LP, Long Y, Xu Y (2021) Butyrate ameliorates alcoholic fatty liver disease via reducing endotoxemia and inhibiting liver gasdermin D-mediated pyroptosis. Ann Transl Med 9:873

Zhang H, Zhao T, Gu J, Tang F, Zhu L (2024) Gut microbiota and inflammasome-mediated pyroptosis: a bibliometric analysis from 2014 to 2023. Front Microbiol 15:1413490

Zhou Z, Xu N, Matei N, McBride DW, Ding Y, Liang H, Tang J, Zhang JH (2021) Sodium butyrate attenuated neuronal apoptosis via GPR41/Gβγ/PI3K/Akt pathway after MCAO in rats. J Cereb Blood Flow Metab 41:267–281